Science of the Total Environment 532 (2015) 556–563

Contents lists available at ScienceDirect

Science of the Total Environment

journal homepage: www.elsevier.com/locate/scitotenv

Formation of complexes between hematite nanoparticles and a non-conventional galactomannan gum. Toward a better understanding on interaction processes

Verónica M. Busch [a,b], Fréderic Loosli [c], Patricio R. Santagapita [a,b], M. Pilar Buera [a,b], Serge Stoll [c,*]

[a] Departamento de Industrias, Facultad de Ciencias Exactas y Naturales, Universidad de Buenos Aires, Intendente Güiraldes 2160, Ciudad Universitaria, C1428EGA Ciudad Autónoma de Buenos Aires, Argentina
[b] Consejo Nacional de Investigaciones Científicas y Técnicas (CONICET), Ciudad Autónoma de Buenos Aires, Argentina
[c] Group of Environmental Physical Chemistry, F.-A. Forel Institute, University of Geneva, 10 route de Suisse, 1290 Versoix, Switzerland

HIGHLIGHTS

- *Vinal* gum has a polydispersity index of 0.65 and a Z-average diameter of 300–450 nm.
- *Vinal* gum and hematite particles have opposite zeta potential values at pH 5.5.
- 0.2–2 mg/L concentration of *vinal* gum promoted aggregation of hematite nanoparticles.
- Different interactions are involved: electrostatic, steric and polymer bridging.

GRAPHICAL ABSTRACT

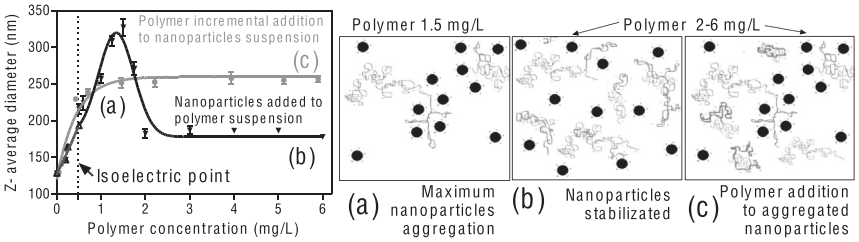

ARTICLE INFO

Article history:
Received 6 April 2015
Received in revised form 30 May 2015
Accepted 30 May 2015
Available online xxxx

Editor: D. Barcelo

Keywords:
Hematite nanoparticles
Vinal gum
Polymer–nanoparticle interaction
Aggregation kinetics
Iron oxides

ABSTRACT

The physicochemical characteristics of hematite nanoparticles related to their size, surface area and reactivity make them useful for many applications, as well as suitable models to study aggregation kinetics. For several applications (such as remediation of contaminated groundwater) it is crucial to maintain the stability of hematite nanoparticle suspensions in order to assure their arrival to the target place. The use of biopolymers has been proposed as a suitable environmentally friendly option to avoid nanoparticle aggregation and assure their stability. The aim of the present work was to investigate the formation of complexes between hematite nanoparticles and a non-conventional galactomannan (*vinal* gum — VG) obtained from *Prosopis ruscifolia* in order to promote hematite nanoparticle coating with a green biopolymer. Zeta potential and size of hematite nanoparticles, VG dispersions and the stability of their mixtures were investigated, as well as the influence of the biopolymer concentration and preparation method. DLS and nanoparticle tracking analysis techniques were used for determining the size and the zeta-potential of the suspensions. VG showed a polydispersed size distribution (300–475 nm Z-average diameter, 0.65 Pdi) and a negative zeta potential (between −1 and −12 mV for pH 2 and 12, respectively). The aggregation of hematite nanoparticles (3.3 mg/L) was induced by the addition of VG at lower concentrations than 2 mg/L (pH 5.5). On the other hand, hematite nanoparticles were stabilized at concentrations of VG higher than 2 mg/L. Several phenomena between hematite nanoparticles and VG were involved: steric effects, electrostatic interactions, charge neutralization, charge inversion and polymer bridging. The process of complexation between hematite nanoparticles and the biopolymer was strongly influenced by the preparation protocols. It was concluded that the aggregation, dispersion, and stability of hematite nanoparticles

* Corresponding author.
E-mail address: serge.stoll@unige.ch (S. Stoll).

http://dx.doi.org/10.1016/j.scitotenv.2015.05.134

depended on biopolymer concentration and also on the way of preparation and initial physicochemical properties of the aqueous system.

1. Introduction

Iron oxide nanoparticles promote rapid degradation of contaminants, reduction of the degradation time by favoring the delivery of suspensions (Comba and Sethi, 2009) and reductive precipitation of metal ions (Li and Zhang, 2007). These properties, which are related to their size, high surface area, the possibility of surface modifications and high reactivity, make them suitable for many applications (Comba and Sethi, 2009; McHenry and Laughlin, 2000). Hematite (α-Fe_2O_3) is one of the several iron oxide polymorphs, like magnetite and maghemite (Xu et al., 2012). Magnetic particles with biocompatible coating have been used for biomedical applications such as in vitro diagnosis, magnetic resonance imaging studies and treatment of some malignant cells, since excess iron could be processed by the body (Berry, 2006). The application of iron oxide particles can be regarded as an innovative technology for the remediation of groundwater contaminated by heavy metal ions and recalcitrant contaminants (Xu et al., 2012; Zhang, 2003). The stability of iron oxide suspensions is crucial in order to assure the arrival to the desired target place and the efficiency of remediation (Dickson et al., 2012).

Hematite nanoparticles (hematite NPs) were found to inverse their surface charge and to enhance their stability by the addition of polysaccharides like guar gum (Tiraferri et al., 2008; Tiraferri and Sethi, 2009), alginate (Chen et al., 2006), Arabic gum (Williams et al., 2006), and carboxymethyl cellulose (He and Shao, 2007). The interaction of hematite NPs with natural organic matter (NOM) has been studied before to investigate the environmental impact of hematite nanoparticles when entering natural aquatic systems (Baalousha, 2009; Nidhin et al., 2012; Palomino and Stoll, 2013). The adsorption of negatively charged humic substances on the positively charged surface of hematite NPs was found to strongly modify their surface charge by inducing charge inversion and thus enhanced their stability through electrostatic repulsion and steric effects. Illés and Tombácz (2006) have found that for a certain natural organic matter concentration the aggregation of iron oxide particles was induced, but at higher NOM concentration the Fe_2O_3 NPs were stabilized. Ferretti et al. (2003) also found that at a given schizophyllan/hematite ratio the flocculation rate was maximum, but the hematite particles were stabilized at higher concentration of polysaccharide. Among the used additives, biopolymers are generally preferred as they are environmentally safe (Nidhin et al., 2012), biodegradable, biocompatible and harmless toward organisms (Comba and Sethi, 2009). In the presence of biopolymers, the inorganic particles (i.e. zero valent iron, hematite or magnetite) have shown to modify their stability and thus their transport properties (Comba and Sethi, 2009; Chen et al., 2006; Nidhin et al., 2012; Tiraferri and Sethi, 2009; Williams et al., 2006; Gómez-Lopera et al., 2001). Many types of interactions have been reported between organic material and inorganic colloids: hydrophobic, electrostatic, van der Waals, ligand exchange, chelation, cation bridging and H-bonding (Philippe and Schaumann, 2014). In some cases, a non-electrostatic stabilization is needed to keep the NP reactivity toward contaminants unaffected for a particular application in targeted systems (Tiraferri et al., 2008; Williams et al., 2006). Galactomannans like guar gum or locust bean gum form solutions which are relatively insensitive to pH changes, addition of electrolytes and heat treatments (Mathur, 2012; Sittikijyothin et al., 2005). The use of green biopolymer as hematite NP coating agent is of great interest. In this sense, the use of the pH-stable galactomannans (Mathur, 2012) extracted from highly available sources offers the possibility to control NP stabilization in a simple way and with less environmental impact. Thus it is necessary to explore innovative and suitable resources for their extraction. A promising biopolymer source is a leguminous plant known as *vinal* (*Prosopis ruscifolia*), from the mesquite family native of North-East Argentina, very abundant in that region, being still an unexploited resource. A galactomannan gum (a sugar polymer of mannose branched with galactose called *vinal* gum (VG)) extracted from *vinal* seeds has similar structure and physicochemical properties as guar gum (Busch et al., 2015). Expanding *vinal* uses will highly impact the local development of innovative materials extracted from natural resources. Considering that the nature and source of the organic material can affect its role while interacting with inorganic colloids, and produce changes in aggregation and sedimentation behaviors (Wilkinson et al., 1997), it is important to study original, innovative biopolymer–inorganic particle interactions and the corresponding complexation processes. The purpose of the present work was to investigate the complex formation and interactions between hematite NPs and a galactomannan gum obtained from *vinal* (*P. ruscifolia*). The resulting changes of the hematite NP surface charges and Z-average diameters as a function of a green biopolymer concentration, dispersion stability and aggregation conditions were considered.

2. Materials and methods

2.1. Materials

Sodium hydroxide (Titrisol 1 M®, Merck & Co. Inc., NJ, USA), ethanol absolute (Biopack, Sistemas Analíticos S.A., Zárate, Argentina), HCl (analytical grade — Sigma Aldrich Co., St. Louis, MO, USA) were used. All water solutions were prepared with MilliQ water with a minimum resistivity of 18 $M\cdot\Omega\cdot cm^{-1}$.

2.2. Hematite synthesis

5.408 g of $FeCl_3\cdot 6\ H_2O$ were added to 2 L of 0.02 M HCl solution at 98 °C. The solution was kept at 98 °C for 10 days (He et al., 2008; Schwertmann and Cornell, 1991). Then, it was cooled to 25 °C and dialyzed with SpectrumLabs Spectra/Por 12–14 kDa dialysis membrane in order to remove the ions. A final hematite NP suspension of 1.64 ± 0.04 g/L was obtained by using the molar extinction coefficient equal to $4.06 * 10^3\ M^{-1}\cdot cm^{-1}$ at 385 nm (Schwertmann and Cornell, 1991) within a HACH Lange DR-3800 spectrophotometer (HACH Lange, Derio Vizcaya, Spain). The NPs were stored as a 0.2 g/L suspension in a cold and dark environment. After image analysis of more than 50 SEM pictures by Palomino and Stoll (2013), the mean SEM diameter of the individual nanoparticles was found equal to 53 ± 5 nm confirming that the nanoparticle sizes were reasonably monodispersed. The Z-average hydrodynamic diameter was found equal to 94 ± 3 nm at pH = 3, indicating the presence of dimmers and trimers in solution.

2.3. Separation of seeds and extraction of vinal gum

Vinal (*P. ruscifolia*) seeds were separated by milling the pods (from Formosa province, Argentina, in 2010) and passing the obtained product through sieves (Sonytest, Rey & Ronzoni S.R.L., Buenos Aires, Argentina). Then, the endosperm (20 g seeds) was manually separated after alkaline treatment (Chaires-Martínez et al., 2008) and stirred in 100 mL of double distilled water for 24 h. After 3 min at 4500 rpm centrifugation, the supernatant was poured into 200 mL of absolute ethanol and the biopolymer flocculated during the storage in the refrigerator (8 °C) for 3 h. VG was then manually separated, dry in oven at 25 °C (300 mbar) for 24 h, and further purified by solubilizing in 50 mL of double distilled water and

another precipitation in ethanol. The obtained VG was dried in a vacuum oven at 25 °C (300 mbar) for 24 h to remove the ethanol and then was freeze-dried by using a Heto Holten A/S, cooling trap model CT 110 freeze-dryer (Heto Lab Equipment, Alleroed, Denmark) operating at a condenser plate temperature of −111 °C, a chamber pressure of 30 Pa, and shelf temperature of 25 °C. VG has molecular weights of $1.43 \pm 0.04 * 10^6$ Da (viscometric) and of $0.73 \pm 0.03 * 10^5$ Da (average number), a mannose/galactose ratio determined by GC–MS of 1.6 and an apparent viscosity of 600 cP at 0.1% (w/v) (Busch et al., 2015). The pK_a value of VG, obtained by titration with a 10^{-3} M solution of sodium hydroxide, was of 6.5 ± 0.5.

2.4. Preparation of suspension of VG and hematite NPs

Hematite NP suspensions were prepared by adding 0.67 mL of the 0.2 g/L stock solution to 39.3 mL of MilliQ water and stirring 30 min at 500 rpm. Final concentration of hematite NP suspensions were 3.30 ± 0.01 mg/L ($6.4 * 10^{12}$ particles/L) for dynamic light scattering (DLS) measurements and 0.33 ± 0.01 mg/L ($6.4 * 10^{11}$ particles/L) for nanoparticle tracking analysis (NTA) measurements. The dilution for NTA measurement was done by adding 5 mL of the 3.30 ± 0.01 mg/L hematite NP dispersion in a 50 mL flask, filling with MilliQ water and stirring 30 min at 500 rpm. Suspensions of VG were prepared by stirring 102.6 ± 0.1 mg of VG in 1 L of MilliQ water for 24 h, and then were sonicated in a Ultrasonic Cleaner Testlab Tb02TA (Instrumental Group S.A., Buenos Aires, Argentina) twice for 30 min. This stock suspension was conserved at 8 °C for further utilization. Dilutions were done through addition of the required amount of the stock suspension of VG to MilliQ water, and stirring at 500 rpm for 30 min.

For increasing or decreasing pH measurements, the adjustment of the pH of the different hematite NPs, VG or mixed solutions was done by the addition of 0.1 or 0.01 M NaOH or HCl solutions. The measurement of pH was performed by a Metrohm 744 pH meter with an electrode Solitrode Pt 1000 (Metrohm AG, Ionenstrasse, Switzerland). The calibration was done with three commercial buffers (pH values of 4, 7 and 10) obtaining a $R^2 > 0.97$ slope.

VG–hematite NP mixtures were prepared by two different ways: i) hematite NP stock solution was added to the previously prepared solution at a specific biopolymer concentration (experiment at fixed concentration — FC), and ii) VG stock solution was sequentially added to a suspension of hematite NPs achieving increasing concentrations of biopolymer (experiment at incremental concentration — IC), and stirring at 500 rpm for 30 min.

2.5. Zeta potential and size measurements

Electrokinetic behavior depends on the potential at the surface of shear between the charged surface and the electrolyte solution. This electrokinetic, called zeta potential, characterizes the electrochemical equilibrium on interfaces and plays an important role on the aggregative stability. It depends on the properties of liquid as well as on properties of the surface. The higher the zeta potential, the stronger the repulsion, the more stable the system becomes (Show, 1966). The hydrodynamic size measured by DLS is defined as the size of a hypothetical hard sphere that diffuses in the same fashion as that of the particle being measured. The Z-average mean is the best value to report when used in a quality control setting and it is the harmonic intensity averaged particle diameter. The polydispersity index (Pdi) is a dimensionless number calculated from a simple 2 parameter fit to the correlation data (the cumulants analysis). Values greater than 0.7 indicate that the sample has a very broad size distribution, and values smaller than 0.05 are rarely seen except for highly monodisperse standards (International Standard ISO13321).

Zeta potential and Z-average diameter values were determined with a Malvern Zetasizer Nano ZS (Malvern Instruments, Malvern, UK) equipped with a 633 nm He–Ne laser and operating with a fixed scattering angle of 173°. After pH was equilibrated, all solutions were stirred at 500 rpm for 15 min before DLS measurements. Stirring time and speed were accurately controlled for measurement reproducibility. 3 measurements of 6 sub-runs of 8 s and 3 measurements of 10 sub-runs were done in automatic mode for size and zeta potential determinations, respectively, at 25 °C. A pause of 5 s between the runs was made in order to stabilize the system before the next measurement. Samples were contained in a disposable polycarbonate cell DTS1060C (Malvern Instruments, Malvern, UK). The calculated ionic power of solutions was in the range of $0.1–0.3 * 10^{-3}$ M.

The time dependence of hematite NP (3.3 mg/L) size was studied by measuring the Z-average diameter at 0, 15, 30, 60, 120 and 225 min. Two different VG concentrations were evaluated: 0.6 mg/L and 6 mg/L. The pH value for this kinetics study was 5.5 ± 0.3.

2.6. Nanoparticle tracking analysis measurements

A NanoSight LM10 (Nanosight Ltd, Salisbury, UK) with NTA was used to determine the size distribution of the prepared dispersions. The NanoSight is a light scattering microscopy device designed to track colloidal particles within the size range of 30–1000 nm (Filipe et al., 2010). All measurements were made at 25 °C, by acquiring 25 frames per second for 1 min, with a drift velocity between 326 and 1334 nm/s and camera shutter between 11 and 30 ms.

The diffusion coefficient can be measured by tracking particle by particle, and then, through application of the Stokes–Einstein equation, particle size (sphere equivalent hydrodynamic diameter) can be determined. NTA has probed to complement DLS technique as it allows the direct observation of the particles, has a better peak resolution, could be applied on both monodisperse and polydisperse systems, and it has a very broad range of diameter ratio population without losing accuracy (Filipe et al., 2010).

As the NTA requires a more dilute range of concentration, each solution was diluted by a factor of 10. Although concentration can modify the distance between particles (He et al., 2008), the VG and hematite NP ratio was kept constant in each system, and the behavior of systems of two polymer–hematite ratios was investigated by both DLS and NTA techniques.

3. Results and discussion

3.1. Hematite NP characterization

Fig. 1 (a and b) shows the zeta potential and size of hematite NPs in water dispersions (without biopolymer). Zeta potential (Fig. 1a) was measured by increasing pH from 2 to 12. The pH value at which the charges are neutralized (point of zero charge or PZC) was found equal to 6.3 ± 0.1. Several authors observed that the hematite PZC was strongly dependent on the size or crystalline phase of the synthesized NPs, and thus Fe_2O_3 PZC were found in the range of 5.5–9.5 (Dickson et al., 2012; He et al., 2008; Nidhin et al., 2012; Palomino and Stoll, 2013). These differences between PZC values were also attributed to synthesis and storage conditions, presence of impurities, and slow aging of the dispersions (i.e. dissolution, aggregation, precipitation) (Cromières et al., 2002). Such results demonstrate the importance of systematic nanoparticle dispersion characterizations prior conducting further experiments.

The hematite NP size was analyzed as the Z-average diameter (Fig. 1b) and was studied by increasing (from 2 to 10) and decreasing pH (from 12 to 4). Starting from extreme pH values, the hematite NPs were either positively or negatively charged (according to the data of Fig. 1a). Upon increasing or decreasing pH their size remained between 100–120 nm up to points close to the PZC region, at pH values around 5 and 8 (delimited by the gray area in Fig. 1). In this region the hematite NP size increased up to 411 nm in the increasing pH experiment, or up to 611 nm in the decreasing pH experiment. The increase of particle

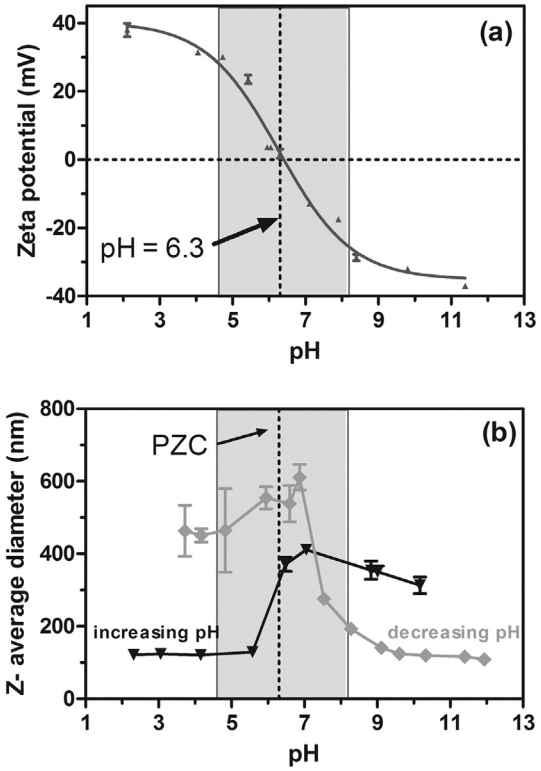

Fig. 1. Zeta potential measurements of hematite NPs by increasing pH (a) and hematite NP Z-average hydrodynamic diameter studied by increasing and decreasing pH (b). The hematite NP (3.3 mg/L) systems were stirred for 15 min at 500 rpm after pH equilibration. PZC: point of zero charge. The gray zone indicates the range of pH corresponding to a zeta potential of 0 ± 25 mV. Bars represent standard deviation values.

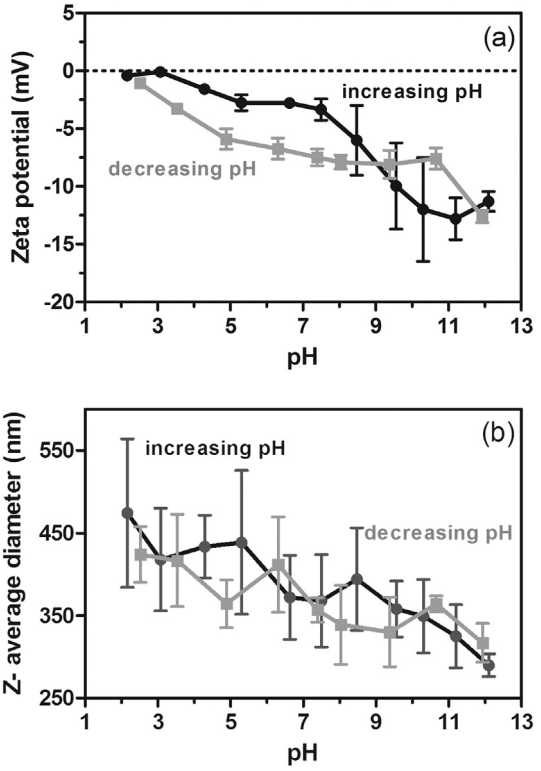

Fig. 2. Zeta potential (a) and Z-average hydrodynamic diameter values (b) of *vinal* gum at 100 mg/L in water as a function of pH. The systems were stirred for 15 min at 500 rpm after pH equilibration. Black circles and gray squares represent the values obtained by a pH titration process from 2 to 12 and from 12 to 2, respectively. Bars represent standard deviation values.

size close to the PZC can be explained by the reduction of the electrostatic repulsive forces (weaker at this point), and consequently the predominance of the van der Waals attractive forces (Cromières et al., 2002). These results agreed with other authors who have found the largest size of hematite aggregates in colloidal systems at pH values between 6 and 10 (Baalousha, 2009; Tombácz et al., 2004).

As shown in Fig. 1b, the aggregation of hematite NPs is not totally reversible: by performing titration curves from acid to alkali and vice-versa, it was observed that when passing through the PZC, further addition of acid or alkali promoted a limited size decrease, but up to about 300–500 nm (instead of the original particle size out of the PZC of about 100–120 nm). The forces that predominate during the aggregation process (van der Waals and hydrophobic) showed to be strong enough to prevent disaggregation and compete with the increasing electrostatic forces during the addition of acid or alkali. As shown in Palomino and Stoll, 2013 the surface charging process and charge inversion of the hematite NPs and aggregates are not strong enough to re-disperse the aggregates. Z-average diameter variations were found different starting from different pH due to the formation of large aggregates when the PZC region was reached. As shown by Palomino and Stoll (2013), the zeta potential was not found to exhibit hysteresis by increasing or decreasing the pH values. This indicates that the hematite charging process is not dependent on the aggregate formation.

3.2. Characterization of vinal gum dispersions

Fig. 2 shows the zeta potential (Fig. 2a) and Z-average diameter values (Fig. 2b) of a 100.0 ± 0.1 mg/L dispersion particles, obtained at increasing and decreasing pH titration experiments (from pH values from 2 to 12 and vice-versa). The zeta potential of VG showed negative values, being more negative at higher pH. This behavior was expected, since VG is a galactomannan like guar gum (Tiraferri et al., 2008) and locust bean gum (Haddarah et al., 2014), which has weak acid behavior in solution, since the main functionality are hydroxyl groups. The pK_a value of VG, obtained by titration with NaOH, was of 6.5 ± 0.5.

The negative charges promote intermolecular electrostatic repulsions between biopolymer chains. In the case of the increasing pH titration curve this fact could lead to dis-agglomeration of some polymer chains which were aggregated at lower pH values. It should also be noted that the change of pH can modify the conformation of polymers; for instance, a more acidic media may promote random coil shape and aggregation of galactomannan (Mathur, 2012) hence increasing the Z-average diameter if the aggregation process is predominant.

As stated before, by increasing the pH value, the zeta potential was found to be more negative in good agreement with the acid–base properties of *vinal* gum. A certain hysteresis in the zeta potential variation was found when increasing and decreasing the pH that could be attributed to the kinetics involved in the changes of conformation at the biopolymer surface, importance of aggregation effects and kinetics aspects related to the acid−base protonation and deprotonation effects. These changes are not instantaneous, and involve several kinds of interactions such as electrostatic, van der Waals, and hydrophobic (Jiang et al., 2009). On the other hand no significant Z-average diameter difference was found between the two curves (Fig. 2b). VG showed a high Pdi of 0.65 ± 0.05 in the analyzed pH range. This high polydispersion strongly influences the Z-average values, leading to higher uncertainty in the mean. A significant decrease of the Z-average was observed due to the charging process of the *vinal* gum chains and dis-agglomeration of aggregates composed of *vinal* gum chains.

3.3. Hematite NP stability as a function of vinal gum concentration

The adsorption of biopolymers on metal oxide NPs modifies the surface charge of the NPs and thus the zeta potential values (Mhlanga et al., 2012). In order to study the interactions between hematite NPs and VG, zeta potential and particle size were investigated as a function of VG concentration at pH 5.5. This pH value was chosen with the aim of promoting electrostatic interactions between positively charged hematite NPs and negatively charged VG. The systems were prepared in two different ways: i) hematite NPs were added to several previously prepared solutions at different biopolymer concentrations (experiment at fixed concentration — FC), and ii) VG was sequentially added to a suspension of hematite NPs achieving increasing concentrations of biopolymer (experiment at incremental concentration — IC).

The obtained zeta potential and particle Z-average hydrodynamic diameter values for the hematite NPs suspended in VG are shown in Fig. 3 (a and b, respectively).

Fig. 3a shows that in both experiments (incremental and at fixed concentration) the zeta potential decreased as the concentration of VG increased due to the adsorption onto hematite NPs. At concentrations above 2 mg/L the zeta potential for both experiments appeared stabilized and did not change with a further increment on polymer concentration. However, in the FC experiment the zeta potential acquired more negative values than in the IC experiment at VG concentrations higher than 1 mg/L, even though hematite NPs were overcharged in both FC and IC experiments. Comba and Sethi (2009) observed the same effect for zero-valent iron NPs in the presence of xanthan gum, and attributed this difference to kinetics, steric and electrostatic effects but also chain relaxation effects related to the biopolymer adsorption on hematite NPs in particular when IC experiments are considered. Then, it could be proposed that less surface area is available for polymer adsorption as the aggregate size is increasing (IC experiment), adsorbing less VG on the surface, being the resulting zeta potential values less negative in IC experiment than in the FC one.

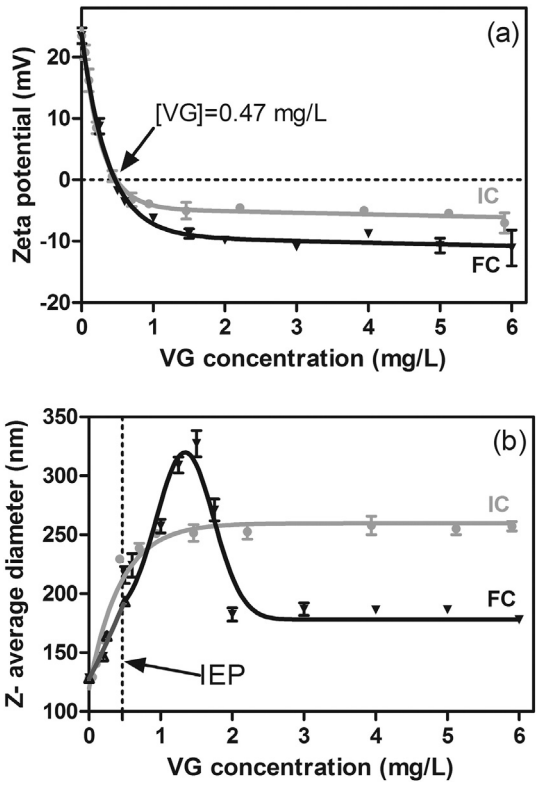

Fig. 3. Zeta potential (a) and Z-average hydrodynamic diameter (b) of hematite NPs as a function of VG biopolymer concentration at pH 5.5. The dotted lines correspond to the isoelectric point (IEP). ▼ values obtained by hematite NP addition to a fixed concentration of VG (FC), ● values obtained by adding incrementally VG (incremental concentration—IC) to a suspension of hematite NPs. The hematite NP concentration in both experiments was maintained constant at 3.3 mg/L. Bars represent standard deviation values.

The difference between FC and IC experiments is also observed on the Z-average diameter values (Fig. 3b). In the FC experiment, NPs showed larger diameters than the NPs without VG (130 nm) at a VG concentration of 0.2–2 mg/L, arriving up to 320 nm at VG concentration of 1.5 mg/L. However, for the 2–6 mg/L range the size of NPs was constant with a Z-average diameter of 184 ± 5 nm (FC experiment). The FC experiment shows that a 2 mg/L VG concentration is enough to prevent aggregation of hematite NPs and stabilize them sterically. In this way, the long loops and tails of the biopolymer extend out into solution (no time for polymer relaxation), leading to steric stabilization. Tiraferri et al. (2008) indicated that systems that are sterically stabilized tend to remain well-dispersed even under conditions at which the zeta potential of the surfaces is significantly reduced. These authors observed that guar gum stabilized nanoscale zero-valent iron NPs preventing NP aggregation, reducing the hydrodynamic radius of bare NPs (154 mg/L) from 500 to 200 nm, by using >0.5 g/L of guar gum. Baalousha (2009) also found that disaggregation of iron oxide aggregates occurred at a given concentration of humic acids due to electrostatic repulsion and steric interactions. Wilkinson et al. (1997) found that the charge neutralization and the stabilization of particles exposed to natural organic matter depended on size, charge and rigidity of the various groups of the present organic macromolecules. It has to be noted that the maximum Z-average diameter (FC experiment) is not coincident with the isoelectric point (VG = 0.47 mg/L). In addition to the charge neutralization process, other mechanisms must be involved during NP aggregation, such as conformational changes of the biopolymer leading to bridging after neutralization, or VG–NP interactions such as hydrogen bonding, as suggested for guar and locust bean gums (Wang and Somasundaran, 2007). In the IC experiment, the hematite NP diameter increased as the VG concentration was increased to 2 mg/L, and then it was kept constant at 250 nm up to at least 6 mg/L of VG. This fact shows that once hematite NP aggregates are formed, they did not disaggregate by a further VG addition (at least in the experiment timeframe of 30 min).

Results shown in Fig. 3 (a and b) indicated that the zeta potential and particle size of hematite NPs suspended in VG will be different if they are added to a VG suspension than if the VG suspension is added to hematite NPs. Such results are also found in good agreement with the findings of Loosli et al. (2015). Using isothermal titration calorimetry they found that the mixing procedure between TiO_2 nanoparticles and alginate polysaccharide chains was playing key roles in the complexation mechanisms.

Fig. 4 shows a scheme of the potential hematite NP adsorption and interaction with VG in both FC and IC experiments. Fig. 4a schematizes the situation at VG concentrations lower than the stabilized size (which is reached at about 2 mg/L, according to Fig. 3b), in both FC and IC experiments: hematite NP aggregation is promoted through interactions with polymer chains. At a VG concentration higher than 2 mg/L, the behavior is different in both experiments. In the FC experiment an initially high VG concentration (2–6 mg/L) leads to stabilization of the size of the hematite NPs (Fig. 4b). While, in the IC experiment (Fig. 4c) further addition of VG to the already aggregated NPs does not promote size decrease at VG concentrations higher than 2 mg/L (Fig. 3b). Besides, the charge neutralization process of the aggregated in the IC experiment induced a less negative zeta potential than in the FC experiments, in which the NPs are less aggregated.

The observed phenomena have important practical consequences. For instance, hematite NPs have a different behavior depending on if they are added to a VG suspension or VG is added to a hematite NP system. Thus, the NP properties will depend on the preparation protocol and mixing procedure. It has to be taken into account that the initial physicochemical properties of the aqueous system have to be previously determined, since they strongly influence the applicability as a remediation strategy.

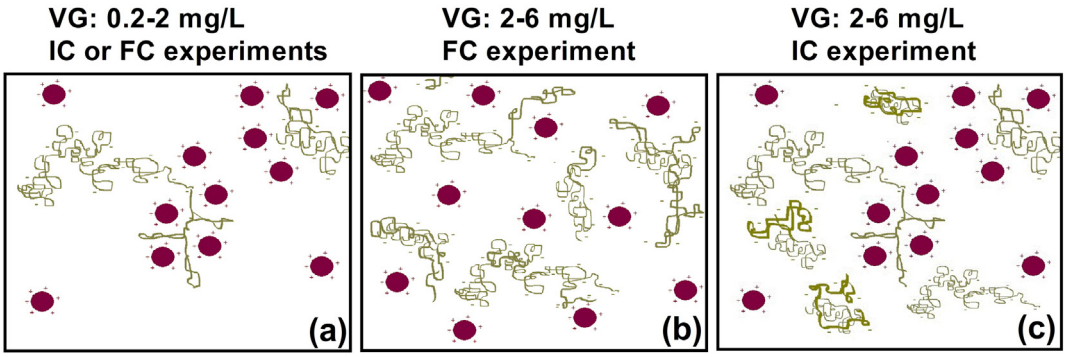

Fig. 4. Schematic stability diagrams of hematite NPs (black circles, positively charged) in different concentrations of *vinal* gum (VG, in gray, negatively charged). Hematite NPs and polymer chain sizes are not at scale. (a) Hematite NP aggregation is promoted by charge neutralization and large aggregates are formed with VG concentration 0.2–2 mg/L for IC and FC experiments of Fig. 3; (b) hematite NPs are stabilized by steric and electrostatic repulsion if higher concentration of VG (>2 mg/L) was initially added (FC experiment); and (c) hematite NP aggregates remain unchanged with further addition of polymer (IC experiment at concentration >2 mg/L).

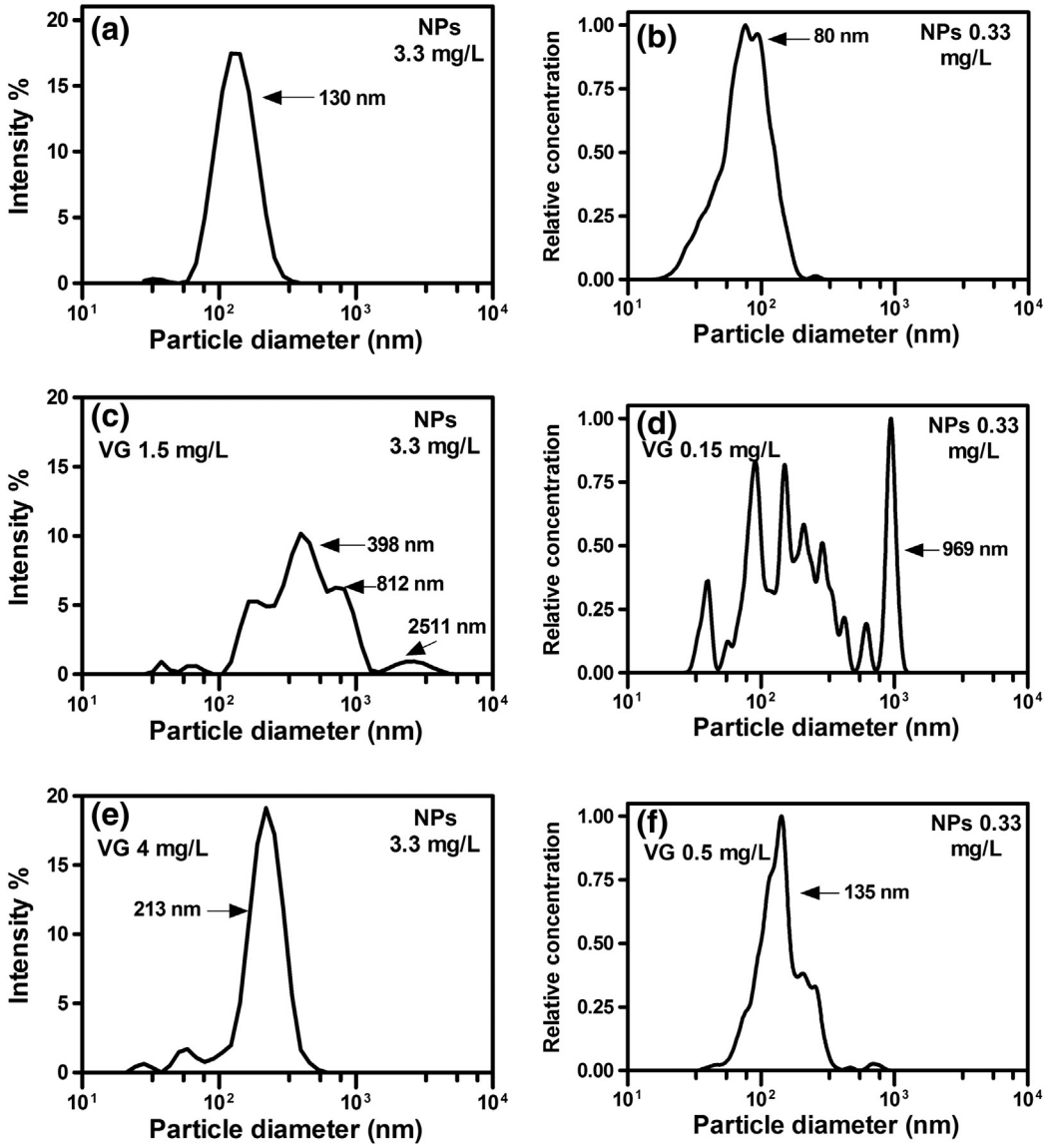

Fig. 5. Intensity/relative concentration vs. particle diameter obtained by dynamic light scattering and nanoparticle tracking analysis (left and right figures, respectively). (a, b) Hematite NPs (c–f) two mixtures of hematite NPs and VG: one at which the aggregation of NPs is promoted (c, d) and the other at excess of VG at which hematite NP size is stabilized (e, f). Arrows point out the maximum of peaks.

Fig. 5 shows intensity/relative concentration vs. particle diameter of hematite NPs (a and b) and of VG–NP mixtures (c–f), analyzed by DLS and NTA. In Fig. 5a and b the hematite NP concentrations used were 3.3 (for DLS analysis) and 0.33 mg/L (for NTA analysis), respectively. It should be noted that diluted samples are required for NTA analysis. However, the hematite NP:VG ratios were maintained for both DLS and NTA analysis. NPs (Fig. 5a and b) behave as a monodisperse system (Pdi of 0.21 ± 0.1), with maximum at 130 nm (DLS) and 80 nm (NTA). This size difference and higher size measured by DLS is explained by the fact that size distribution obtained by DLS is intensity weighted while the size distribution obtained by NTA is number based.

Considering the experiment at fixed concentration (FC), two different conditions were analyzed: VG concentration at which hematite NP aggregation is favored (up to 2 mg/L), and at VG concentration higher than 2 mg/L (at which the size seems to be stabilized between 150 and 200 nm, as previously discussed in relation to Fig. 3b). Fig. 5 (c–f) shows the size distribution of hematite NP–VG mixtures in the two mentioned conditions. Fig. 5c and d shows that at the VG concentration where NP aggregation is promoted, the NP–VG system is quite polydispersed (Pdi of 0.4 ± 0.1) and aggregated, according to the obtained size by both techniques. On the other hand, at higher concentration of VG the hematite NPs were monodispersed (Fig. 5e and f), showing smaller diameters than in the previous situation (Fig. 5c and d). An increment of the size of hematite NPs due to the addition of a polymer (alginate) has been reported by Chen et al. (2006), attributed to the adsorption of the polymer onto NP surface. NTA videos of hematite NPs (Video 1) and hematite NPs at two different polymer concentrations (Videos 2 and 3) were included in the additional material. At a VG concentration of 0.5 mg/L and hematite NPs at 0.33 mg/L, a high number of particles with fast movements could be observed (Video 3, corresponding to Fig. 5f), confirming their small size. At lower concentration of VG (0.15 mg/L) and the same concentration of hematite NPs, fewer particles with slower movements can be seen (Video 2, corresponding to Fig. 5d). For many applications, such as for water remediation purposes, it is important that particle size remains constant over time (Dickson et al., 2012). Thus, the aggregation kinetics of hematite NPs is a central practical point. Z-average diameter was studied as a function of time at two different fixed VG concentrations, as shown in Fig. 6. These concentrations were chosen according to Fig. 3b in order to provide information of the hematite NPs at low and high VG concentrations. As expected, there were no differences in the initial hematite NP size for both systems (130 nm). The curves observed in Fig. 6 showed two different behaviors, according to the VG concentration range. During the first 15 min, at a VG concentration of 0.6 mg/L (close to the isoelectric point, Fig. 3b) the NP size increased from 129 ± 3 to 274 ± 6 nm and then continued to undergo slow aggregation reaching a Z-average diameter value of 381 ± 19 nm (at t = 330 min). Instead, at a VG concentration of 6 mg/L they increased from 129 ± 3 to 191 ± 4 nm, they stabilized their size at 100 min and remained constant (at about 210 nm) in all the time-frame of the experiment. Thus, at the lowest VG concentration the aggregation was promoted as the surface charges were neutralized, leading to hematite NP aggregation and possible bridging of the polymer chains. The hematite NPs with the higher VG concentration had a lower global growth rate. This could be attributed to polymer adsorption and further stabilization of hematite NPs, as previously discussed in relation to Figs. 3 and 5.

Finally, it is important to analyze an apparent discrepancy, which is explained by the stability conferred by VG. The zeta potential at pH 5.5 ± 0.3 (Fig. 1a) is of larger magnitude for bare particles than it is for particles coated with VG (Fig. 3a), which could lead to stronger electrostatic repulsion and finally to a higher stability of the particle suspensions. However, the additional stabilization conferred by VG through direct interaction (hydrogen bonding) provoked a steric stabilization, allowing the system to remain well-dispersed (Fig. 6.) even under conditions where the zeta potential of the surfaces is significantly reduced.

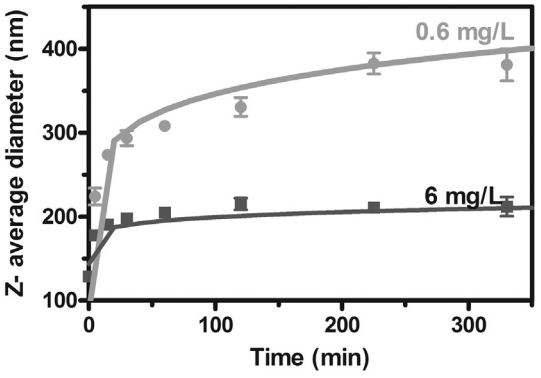

Fig. 6. Z-average diameter of hematite NPs (3.3 mg/L) as a function of time in the presence of different VG concentrations: 0.6 mg/L and 6 mg/L. Bars represent standard deviation values. Lines are only indicative.

4. Conclusions

- The particle Z-average diameter and zeta potential of VG, a polymer from non-conventional sources, was characterized for the first time as a function of pH at low concentrations. *Vinal* gum showed similar characteristics as other galactomannan gums (locust bean gum or guar gum) being highly polydispersed (Pdi equal to 0.65 ± 0.05) and having negative zeta potential values for pH values between 2 and 12.
- The aggregation and/or stability of hematite NP systems depended on VG concentration.
- Aggregation and dispersibility of hematite NPs depend on the way of preparation: the addition of hematite NPs to VG dispersions showed a different behavior than the addition of VG to dispersed hematite NPs.
- The application of hematite NPs as a remediation strategy requires both strict control of the polymer and NP suspensions and the knowledge of the target aqueous system physicochemical properties.
- At the lower VG concentration range (between 0.2 and 2 mg/L), aggregation of hematite NPs is promoted. At higher VG concentrations (from 2 mg/L up to 6 mg/L), hematite NPs were stabilized.
- Several phenomena seem to be involved in hematite NP interactions with VG: steric, electrostatic, charge neutralization and inversion, and bridging of polymer chains.

Supplementary data to this article can be found online at http://dx.doi.org/10.1016/j.scitotenv.2015.05.134.

Acknowledgments

The authors are indebted to Ing. Ana Rentería, Ing. Manuel Palacio and the Universidad de Santiago del Estero for collecting and donating *vinal* pods. We acknowledge CONICET (PIP 100846), UBACyT (20020100100397), and ANPCyT (PICT 2008–0928). Lic. Verónica Busch is grateful to Coimbra Group, the University of Geneva and Institute Forel, for the Scholarship of the program for Young Professors and Researchers from Latin American Universities.

References

Baalousha, M., 2009. Aggregation and disaggregation of iron oxide nanoparticles: influence of particle concentration, pH and natural organic matter. Sci. Total Environ. 407, 2093–2101. http://dx.doi.org/10.1016/jscitotenv.2008.11022.

Berry, C., 2006. Possible exploitation of magnetic nanoparticle–cell interaction for biomedical applications. J. Mater. Chem. 15, 543–547.

Busch, V.M., Kolender, A.A., Santagapita, P.R., Buera, M.P., 2015. *Vinal* gum, a galactomannan from *Prosopis ruscifolia* seeds: physicochemical characterization. Food Hydrocoll. http://dx.doi.org/10.1016/j.foodhyd.2015.04.035.

Chaires-Martínez, L., Salazar-Montoya, J.A., Ramos-Ramírez, E.G., 2008. Physicochemical and functional characterization of the galactomannan obtained from mesquite seeds (*Prosopis pallida*). Eur. Food Res. Technol. 227, 1669–1676.

Chen, K.L., Mylon, S.E., Elimelech, M., 2006. Aggregation kinetics of alginate-coated hematite nanoparticles in monovalent and divalent electrolytes. Environ. Sci. Technol. 40 (5), 1516–1523.

Comba, S., Sethi, R., 2009. Stabilization of highly concentrated suspensions of iron nanoparticles using shear-thinning gels of xanthan gum. Water Res. 43, 3117–3726.

Cromières, L., Moulin, V., Fourest, B., Giffaut, E., 2002. Physico-chemical characterization of the colloidal hematite/water interface: experimentation and modeling. Colloids Surf. A 202, 101–115.

Dickson, D., Liu, G., Li, C., Tachiev, G., Cai, Y., 2012. Dispersion and stability of bare hematite nanoparticles: effect of dispersion tools, nanoparticle concentration, humic acid and ionic strength. Sci. Total Environ. 419, 170–177.

Ferretti, R., Stoll, S., Zhang, J., Buffle, J., 2003. Flocculation of hematite particles by a comparatively large rigid polysaccharide: schizophyllan. J. Colloid Interface Sci. 266, 328–338.

Filipe, V., Hawe, A., Jiskoot, W., 2010. Critical evaluation of nanoparticle tracking analysis (NTA) by nanosight for the measurement of nanoparticles and protein aggregates. Pharm. Res. 27, 796–810.

Gómez-Lopera, S.A., Plaza, R.C., Delgado, A.V., 2001. Synthesis and characterization of spherical magnetite/biodegradable polymer composite particles. J. Colloid Interface Sci. 240, 40–47.

Haddarah, A., Bassal, A., Ismail, A., Gaiani, C., Ioannou, I., Charbonnel, C., Hamieh, T., Ghoul, M., 2014. The structural characteristics and rheological properties of Lebanese locust bean gum. J. Food Eng. 120, 204–214.

He, F., Shao, D., 2007. Manipulating the size and dispersibility of zerovalent iron nanoparticles by use of carboxymethyl cellulose stabilizers. Environ. Sci. Technol. 41 (17), 6216–6221.

He, Y.T., Wan, J., Tokunaga, T., 2008. Kinetic stability of hematite nanoparticles: the effect of particle size. J. Nanoparticle Res. 10, 321–332. http://dx.doi.org/10.1007/s11051-007-9255-1.

Illés, E., Tombácz, E., 2006. The effect of humic acid adsorption on pH-dependent surface charging and aggregation of magnetite nanoparticles. J. Colloid Interface Sci. 295, 115–123.

International Standard ISO13321, 1996. Methods for Determination of Particle Size Distribution Part 8: Photon Correlation Spectroscopy. International Organisation for Standardisation (ISO).

Jiang, J.S., Gan, Z.F., Yang, Y., Du, B., Qian, M., Zhang, P., 2009. A novel magnetic fluid based on starch-coated magnetite nanoparticles functionalized with homing peptide. J. Nanoparticle Res. 11, 1321–1330.

Li, X., Zhang, W., 2007. Sequestration of metal cations with zerovalent iron nanoparticles —A study with high resolution X-ray Photoelectron Spectroscopy (HR-XPS). J. Phys. Chem. C 111, 6939–6946.

Loosli, F., Vitorazi, L., Berret, J.-F., Stoll, S., 2015. Towards a better understanding on agglomeration mechanisms and thermodynamic properties of TiO_2 nanoparticles interacting with natural organic matter. Water Res. 80, 139–148.

Mathur, N.K., 2012. Industrial Galactomannan Polysaccharides. CRC Press Taylor & Francis Group, Boca Raton.

McHenry, M.E., Laughlin, D.E., 2000. Nano-scale materials development for future magnetic applications. Acta Mater. 48, 223–238.

Mhlanga, S.S., O`Connor, C.T., McFadzean, B., 2012. A study of the relative adsorption of guar onto pure minerals. Miner. Eng. 36–38, 172–178.

Nidhin, M., Sreeram, A.J., Nair, B.U., 2012. Polysaccharide films as templates in the synthesis of hematite nanostructures with special properties. Appl. Surf. Sci. 258, 5179–5184.

Palomino, D., Stoll, S., 2013. Fulvic acids concentration and pH influence on the stability of hematite nanoparticles in aquatic systems. J. Nanoparticle Res. 15, 1428–1436. http://dx.doi.org/10.1007/s11051-013-1428-5.

Philippe, Schaumann, G.E., 2014. Interactions of dissolved organic matter with natural and engineered inorganic colloids: a review. Environ. Sci. Technol. http://dx.doi.org/10.1021/es502342r.

Schwertmann, U., Cornell, R.M., 1991. Iron Oxides in the Laboratory: Preparation and Characterization. Weinheim, VCH.

Show, D., 1966. Introduction to Colloid and Surface Chemistry. Butterworth-Heinemann An imprint of Elsevier Science, Oxford 07506 11820.

Sittikijyothin, W., Torres, D., Gonçalves, M.P., 2005. Modelling the rheological behaviour of galactomannan aqueous solutions. Carbohydr. Polym. 59, 339–350.

Tiraferri, A., Sethi, R., 2009. Enhanced transport of zerovalent iron nanoparticules in saturated porous media by guar gum. J. Nanoparticle Res. 11, 635–645.

Tiraferri, A., Chen, K.L., Sethi, R., Elimelech, M., 2008. Reduced aggregation and sedimentation of zero-valent iron nanoparticles in the presence of guar gum. J. Colloid Interface Sci. 324, 71–79.

Tombácz, E., Libor, Z., Illés, E., Majzika, A., Klumpp, E., 2004. The role of reactive surface sites and complexation by humic acids in the interaction of clay mineral and iron oxide particles. Org. Geochem. 35, 257–267.

Wang, J., Somasundaran, P., 2007. Study of galactomannose interaction with solids using AFM, IR and allied techniques. J. Colloid Interface Sci. 309, 373–383.

Wilkinson, K.J., Joz-Roland, A., Buffle, J., 1997. Different roles of pedogenic fulvic acids and aquagenic biopolymers on colloid aggregation and stability in freshwaters. Limnol. Oceanogr. 42, I714–I1724 (g).

Williams, D.N., Gold, K.A., Holoman, T.R.P., Ehrman, S.H., Wilson Jr., S.O., 2006. Surface modification of magnetic nanoparticles using gum Arabic. J. Nanoparticle Res. 8, 749–753. http://dx.doi.org/10.1007/s11051-006-9084-7.

Xu, P., Zeng, G.M., Huang, D.L., Feng, C.L., Hu, S., Zhao, M.H., 2012. Use of iron oxide nanomaterials in wastewater treatment: a review. Sci. Total Environ. 424, 1–10.

Zhang, W.X., 2003. Nanoscale iron particles for environmental remediation: an overview. J. Nanoparticle Res. 5, 323–332.